Dynamic performance measurements of Na/NiCl$_2$ cells for electric vehicle applications

Jai Prakash [a,*], Laszlo Redey [b], Donald R. Vissers [b]

[a] *Center for Electrochemical Science and the Department of Chemical and Environmental Engineering, Illinois Institute of Technology, 10 W 33rd Street, Chicago, IL 60616, USA*
[b] *Chemical Technology Division, Argonne National Laboratory, Argonne, IL 60439, USA*

Abstract

A method to measure the dynamic-performance of sodium/nickel chloride research cells under various dynamic load profiles, such as the Simplified Federal Urban Driving Schedule (SFUDS) has been described. The dynamic performance of various Na/NiCl$_2$ research cells is measured in various power profiles in which the duration, intensity, and ratios of the power levels (mW/cm^2) in the SFUDS-like profiles are varied. Performance parameters such as area-specific impedance and specific-area energy are obtained by discharging these cells under actual conditions that exist in the full-size battery during the intended applications. The performance parameters measured by this method are employed in relatively simple scale-up calculations to project performances of full-size battery. © 2000 Elsevier Science S.A. All rights reserved.

Keywords: Dynamic performance; Batteries; Nickel chloride; Specific energy; Specific power

1. Introduction

The sodium/nickel chloride cell couple is a very promising sodium/β-alumina battery system [1–11]. The high theoretical specific energy (790 W h/kg), high cell voltage (2.59 V), wide temperature range, cell failure mode, and good cycling characteristics of this battery system have made it a viable candidate for electric vehicle applications. The sodium/nickel chloride cell couple is similar to the Na/S cell in that it uses much of the same technology. For instance, the Na/NiCl$_2$ cell, like the Na/S, uses a liquid sodium negative electrode and the β″-alumina solid electrolyte. However, unlike the sodium/sulfur cell, it uses a secondary electrolyte of molten sodium tetrachloroaluminate (NaAlCl$_4$) in the positive electrode and an insoluble nickel chloride as the active material. The NaAlCl$_4$ electrolyte conducts sodium ions from the β″-Al$_2$O$_3$ electrolyte to the nickel chloride electrode reaction sites. Sodium and Na[AlCl$_4$] are molten at the operational temperature (250°C to 400°C) of the cell.

Na[AlCl$_4$] is added to the porous Ni/NiCl$_2$ electrode to transport Na$^+$ ions from the surface of the β″-alumina electrolyte to the reaction sites at the interior of the positive electrode. The cell reaction is:

$$2Na + NiCl_2 = 2NaCl + Ni.$$
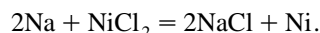
The Na/NiCl$_2$ cells designed for electric vehicle (EV) propulsion must satisfy several demanding requirements. The most important technical requirements are related to high specific energy and peak power, which need to be available during the dynamic load conditions of these applications. The most difficult requirement is the wide dynamic range of electric power needed to propel the electric vehicle in city traffic, which involves frequent changes in speed. Therefore, it is important to understand the dynamic performance of the battery cells under dynamic load conditions that prevail during the electric vehicle propulsion. Experimentation with full-size batteries to find an optimum design that satisfy an electric vehicle's stringent requirements can be very expensive and time-consuming. Consequently, it is useful to have a method that can reliably project the dynamic-performance of various design options and provide a means for selecting the optimum versions without fabricating many design ver-

* Corresponding author. Tel.: +1-312-567-3639; fax: +1-312-567-8874; e-mail: prakash@iit.edu

sions of full-size batteries for testing. The dynamic-performance measuring method can be extremely useful even at the early stage of battery R&D, when systems intended for electric vehicle propulsion are being evaluated [6]. This paper describes a method to measure those dynamic-performance parameters of $Na/NiCl_2$ research cells under dynamic load profiles that prevail during the electric vehicle propulsion.

2. Experimental

Electrochemical investigations of the $Na/NiCl_2$ cell were carried out in an electrochemical research cell (Fig. 1), which closely simulates the components and operational conditions of the full size battery. The capacity of these cells ranged between 1.0 to 1.2 A h. The research cell had a molten sodium negative electrode, a nickel chloride positive electrode, a β''-alumina tube (CSPL, UK) and a molten electrolyte, $Na[AlCl_4]$ (APL Engineered Materials). The molten sodium electrode also served as the reference electrode due to its negligible polarization.

Two types of nickel chloride electrodes were investigated in this study; baseline electrodes with no chemical additives in the positive electrode and improved electrodes with chemical additives in the positive electrode. The electrodes were assembled in the discharged state by mixing of Ni-255 (Novamet Specialty Products) and NaCl powders (Aldrich Chemical) thoroughly and then pressing the material into a 0.5-cm thick pellet with a diameter of 2.80 cm. The pellet was subsequently sintered at 750–890°C under a reducing atmosphere. The improved porous sintered electrode with better morphology was fabricated by mixing 10-wt.% NaBr, 10-wt.% NaI, and 10 wt.% of the ammonium bicarbonate with the Ni-255 and NaCl powders and then pressing the material into a 0.5-cm thick
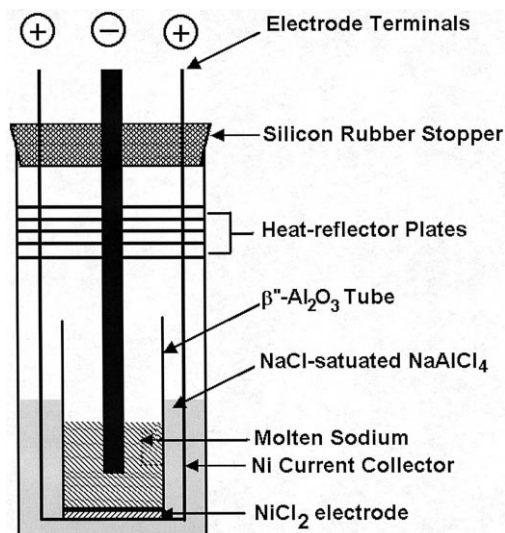
Fig. 1. Schematics of the research cell used for $Na/NiCl_2$ cell studies.
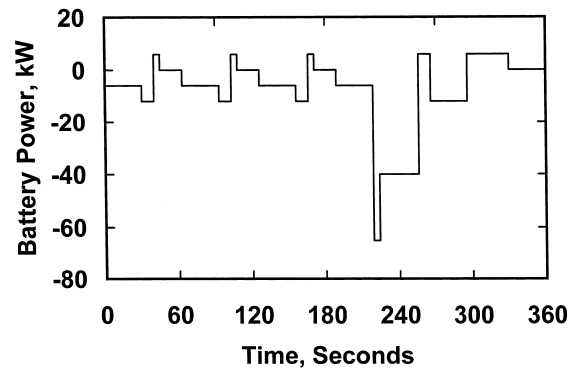
Fig. 2. Specific power levels of an electric vehicle battery based on the SFUDS.

pellet. Sulfur, 2 wt.% by the electrolyte weight was incorporated into the liquid electrolyte. Sulfur was added to stabilize the cell capacity and produce a synergistic effect. This pellet was heated in the furnace first at 150°C for 1 h to decompose ammonium bicarbonate. During the decomposition of the ammonium bicarbonate at 150°C, the ejection of NH_3, CO_2 and H_2O vapors produce better porous structure. The pellet was subsequently sintered at 750–890°C under a reducing atmosphere. After sintering, these electrodes were vacuum impregnated with liquid $Na[AlCl_4]$, and then placed in the cell's positive electrode compartment. The electrochemically active area of the research cell was 6.0 cm^2. The weight of the research cell was about 14 g. The positive electrode compartment contained enough NaCl to saturate the liquid even during fully charged conditions.

A uniform one-dimensional current distribution was maintained in the nickel chloride electrode, which was cycled in the anodic (3.0 V) and cathodic (2.0 V) directions against a Na electrode. In the static measuring mode, the current interruption technique was used during the cycling to evaluate the electrode and cell impedance. In the dynamic measuring mode, either a varying current (galvanodynamic method) or a varying power (powerdynamic method) level was used during the discharge half-cycle. One of these load patterns is the Simplified Federal Urban Driving Schedule (SFUDS), which was developed [12] to mimic the power-load pattern of electric-vehicle batteries. The SFUDS profile defines a dynamic power range, which is characterized by the various discharge-power levels (indicated by negative sign in Fig. 2) and, also, by the power level of the short charge periods that are associated with the regenerative braking of the vehicle (positive values in Fig. 2). The numeric values of the power levels are dictated by the vehicle parameters to provide adequate power for acceleration and cruising. For example, the power levels shown in Fig. 2 are required for a 695-kg battery to propel a 2400-kg curb-weight electric vehicle in city driving [12]. The SFUDS cycles were repeated until the cell voltage drops to a preset value of 2.0 V during the heaviest load step of the SFUDS cycle. To facilitate the
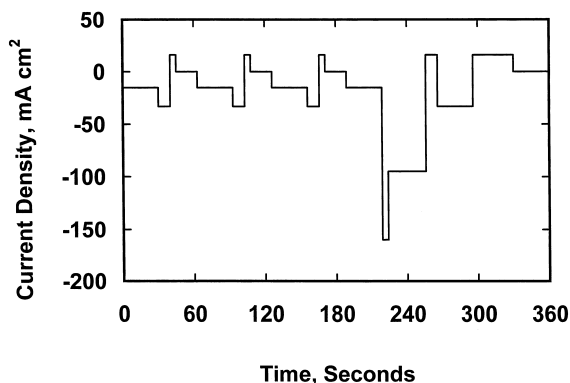
Fig. 3. Constant current steps used in a galvanodynamic SFUDS-like discharge of a Na/NiCl$_2$ research cell.

use of simpler laboratory instrumentation, the constant power steps required by SFUDS were substituted by constant current steps (Fig. 3). The current densities were selected in such a way that the full-size battery (of a particular design) at these current densities would meet the power requirements of the electric vehicle shown in Fig. 2. The required power levels of the SFUDS for a particular vehicle are vehicle-design specific, and the specific power levels of the research cell are cell-design specific and are expressed in units of power (watts) per weight, volume, or area based on the physical parameters of the research cell. The instrumentation and method for these measurements are described in detail elsewhere [13].

3. Results and discussion

The voltage profiles of a Na/NiCl$_2$ cell tested with galvanodynamic pattern (Fig. 3) are shown in Fig. 4 for the 0, 95, and 160 mA/cm^2 load steps at every fifth SFUDS cycle. The curves shown in Fig. 4 provide data to calculate area-specific energy and power at any current or
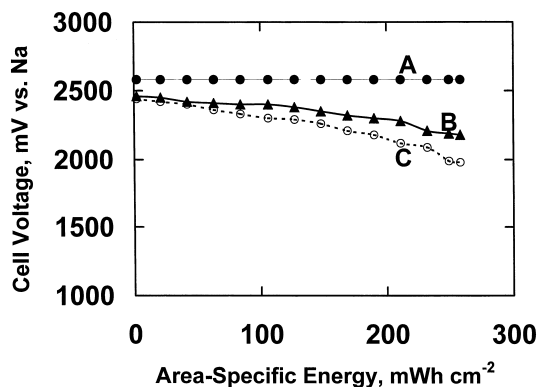
power level. The current densities in the research cell for the section of the SFUDS are selected such a way that the full-size battery (of a particular design) at these current densities would meet the power requirements of the electric vehicle. In this example, the 95 and 160 mA/cm^2 current densities represent the two highest levels of the SFUDS cycle. It was observed that the voltage pattern of the SFUDS discharge greatly varies due to a number of factors. These include the chemistry, microstructure, and fabrication method of the cell electrodes, the condition of cell operation, such as temperature, and compression force, and the actual load-level set of the SFUDS. For instance, in Fig. 5 the voltage response of an improved cell to the same galvanodynamic discharge is compared to that of the baseline cell whose voltage curves are plotted in Fig. 5. A striking difference between the two cells is the substantially different available energies within the same voltage range and power levels under dynamic load conditions. If the SFUDS profile is very demanding for power, a large amount of energy still remains in the battery that is available subsequently at a lower power level. The discharge voltage profiles of the improved nickel chloride electrode discharged under static and dynamic current profiles are given in Fig. 6 for the comparison purposes. It can be seen from this figure that the static discharge and different dynamic discharge profiles produce significant differences in cell performance. The improved electrode fabricated with the chemical additives and a specially tailored show significantly improved performance due to decreased impedance of the nickel chloride layer and optimized pore structure to support effective mass transport. The total discharged energy in the galvanodynamic cycles is more than that available in galvanostatic cycling because of the beneficial effect of the charge sections of the regenerative braking in the SFUDS.

The electric systems of an electric vehicle would accept only a limited variation of the battery voltage during the
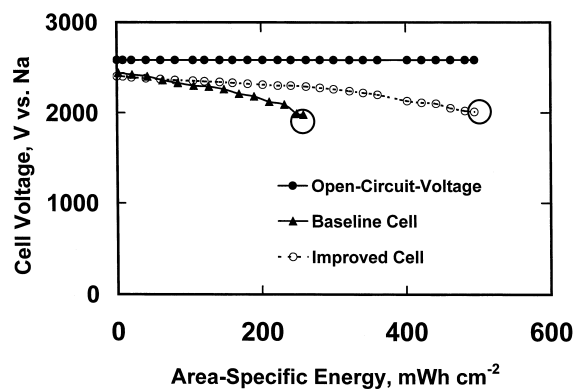

Fig. 4. Voltage response of a baseline Na/NiCl$_2$ research cell to the galvanodynamic discharge profile of Fig. 3 at 300°C. The cell voltages at 0, 95, and 160 mA/cm^2 current density steps are shown for each 5th consecutive SFUDS cycles.

Fig. 5. Voltage response of two Na/NiCl$_2$ research cells to the galvanodynamic discharge to the 5-s long 160 mA/cm^2 current density step at 300°C. Big circles indicate termination of the discharge half-cycle at 2.0 V.
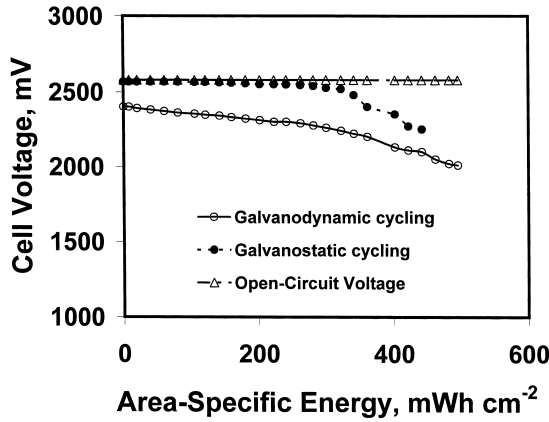
Fig. 6. Effect of additives on the cell voltage and discharge capacity of the Na/NiCl$_2$ cells during the discharge half-cycles at 300°C. The cells were discharged at a constant current density of 20 mA/cm^2.
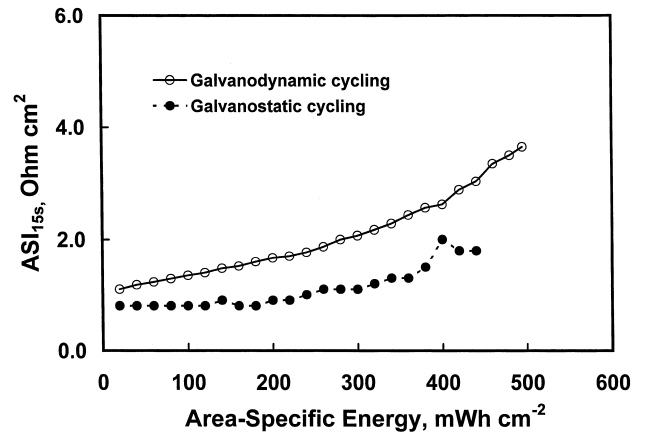

Fig. 8. Area-specific impedance of Na/NiCl$_2$ cells shown in the highest power-demand section for every 5th SFUDS cycle.

operation of the vehicle (including the regenerative breaking) and recharging of the battery. The present electric system may allow a battery voltage variation of not more than ±25% or ±30% relative to the open-circuit voltage of the fully charged battery. This range of the battery voltage is approximately equivalent to a discharge voltage range of 2.6 to 2.0–1.8 V for the investigated Na/NiCl$_2$ research cell. The most critical range of the SFUDS is the one at the highest power level because excessively dropping voltage terminates the discharge according to the above-described limitation, even if substantial capacity is available at a lower power level. The SFUDS discharge cycle sequence is terminated when the cell voltage or power drops to the low cut-off value. These discharge terminations points are marked by big circles for both cells in Fig. 5. As shown in Fig. 5, the improved cell reaches this termination point at a much higher area-specific capacity. A cell that has reached the discharge termination point must be recharged.

The relationship between the performance of the research cells and the full-size battery can be established by modeling and scale-up calculations. A critical parameter for these calculations i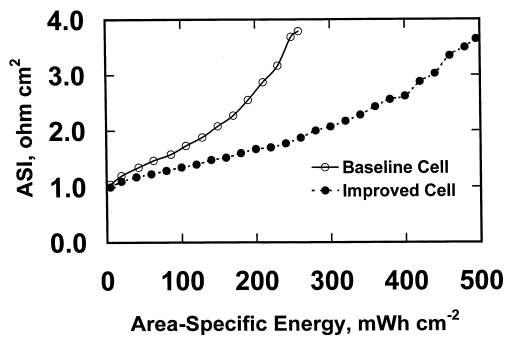s the area-specific impedance of the research cell or its electrodes [14]. Projections for full-size battery performance based on the measurement of the ASI are highly reliable because this calculation uses cell parameters that are measured under the actual conditions of the required applications. The area-specific impedance ASI$_t$ is time-dependent and includes the resistance, capacitance, and inductance components of the electrode. The ASI is a very important property of the electrode in that it provides the nature and the magnitude of the electrochemical and mass-transport limitations. The ASI for a cell or an electrode was calculated from the voltage or potential difference measured between the open- and closed-circuit values. For a dynamically discharged cell, an ASI plot is calculated from the voltage pattern of the cell. Fig. 7 shows the highest power-demand section for every 5th SFUDS cycle for the two Na/NiCl$_2$ cells. Fig. 8 shows a comparison between the area-specific impedance (ASI$_{15s}$) measured by the interrupted galvanostatic and the galvanodynamic methods, as a function of discharged capacity per unit volume for the improved nickel chloride electrodes. It can be seen from Fig. 8 that the values of ASI increase rapidly during SFUDS discharge due to high current pulses.
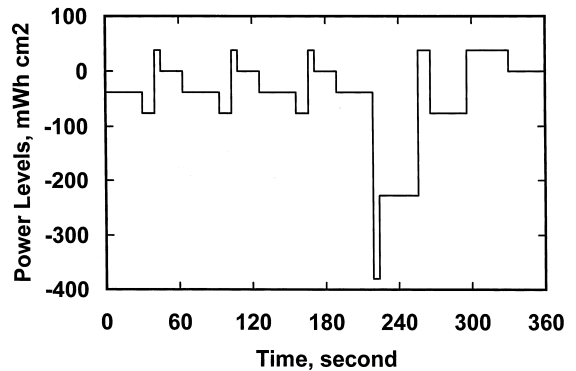

Fig. 7. Effect of additives on the area-specific impedance of the Na/NiCl$_2$ cells during the discharge half-cycles at 300°C. The cells were discharged at a constant current density of 20 mA/cm^2.

Fig. 9. Area-specific power levels of SFUDS cycles used to investigate the effect of power levels on the dynamic performance of the Na/NiCl$_2$ cells.

Table 1
Measured performance of $Na/NiCl_2$ research cell and projections for a 400-kg electric vehicle battery in SFUDS discharge

SFUDS type	Research cell				400-kg battery		
	Power required, mW/cm^2	Discharge limit, V	Measured energy, mW h/cm^2	Energy, kW h	Power, kW	Specific energy, W h/kg	Specific power, W/kg
PD-1	380	1.6	287	49	65	123	162
		1.9	264	45	65	113	162
PD-2	250	1.6	366	60	41	150	103
		1.9	341	56	41	140	103

However, the ASI values remain relatively constant up to 80% depth-of-discharge during constant current discharge. The termination points of the curves at higher utilized capacities indicate increased available energy density (W h/cm^3), and the lowered area-specific impedance of the nickel chloride electrode (Ω cm^2) indicates higher power capability. Use of the chemical additives in the nickel chloride electrode (improved electrode) significantly improve the electrode performance, as shown by the higher available specific energy and the much lower area-specific impedance during SFUDS testing.

The power levels of the high-power-demand sections of the SFUDS were also varied to study the effect of power levels (mW/cm^2) on the available discharged energy. The powerdynamic cycling profile in these measurements (Fig. 9), however, follows the time intervals of the standard SFUDS profile shown in Fig. 2. Table 1 shows the measured discharged energies in two different SFUDS profiles for the $Na/NiCl_2$ baseline cells and the projected performance of a 400-kg full-size battery. These power profiles are characterized by the high power demand for high acceleration for a relatively short time (380 or 250 mW/cm^2 at the end of a 7-s pulse). The discharge in these measurements was terminated when the cell voltage dropped to 1.6 and 1.9 V during the highest power level section of the SFUDS. This table shows that the available area-specific power and energy are greatly influenced by the power levels, voltage cut-off, and time intervals of the dynamic cycle. The power-related numbers, e.g., in Table 1, neither relate to the 80% depth of discharge, nor are the peak power values. The power-related numbers show the actual level of power that the cell or battery can maintain in the specified SFUDS profiles during as many SFUDS cycles that cumulatively produce the discharged energy equal to the respective energy related numbers in the table. The projected performance numbers given here are qualitative in nature and were calculated by assuming a linear relationship between the performance of the research cell and full-size battery. Redey et al. [15] have shown that the area-specific performance value of a properly designed research cell are in linear relationship with the respective performance values of the battery, and a factor can be calculated to establish a numerical relationship between them. An important significance of the results of the present powerdynamic measurements is that they provide us a firm basis to project dynamic-performance parameters for full-size electric vehicle batteries.

4. Conclusions

A method to measure the dynamic-performance of sodium/nickel chloride research cells under various dynamic load profiles that exist in the full-size battery during the intended applications has been described. It is shown that the static discharge and dynamic discharge profiles produce significant differences in cell performance. The measured performance parameters can be employed in relatively simple scale-up calculations to project performances of full-size battery. This method is very useful for R&D of various battery systems and provides an expedient means for reliable performance projections. Considerable time and cost savings can also be achieved because the method minimizes the need for fabrication of and experimentation with full-size cell design options.

Acknowledgements

References

[1] D. Sahm, J.L. Sudworth, in: Proceedings of DOE/EPRI Beta Battery Workshop, Vol. VIII, 1991, p. 31.
[2] L. Redey, D.R. Vissers, J. Prakash, U.S. Patent No. 5,283,135 (1994).
[3] L. Redey, D.R. Vissers, J. Prakash, U.S. Patent No. 5,340,668 (1994).
[4] L. Redey, D.R. Vissers, J. Prakash, K.M. Myles, U.S. Patent No. 5,532,078 (1996).
[5] L. Redey, D.R. Vissers, J. Prakash, K.M. Myles, U.S. Patent No. 5,536,593 (1996).

[6] R.J. Bones, D.A. Teagle, S.D. Brooker, F.L. Cullen, J. Electrochem. Soc. 136 (1989) 1274.

[7] B.V. Ratnakumar, S. Di Stefano, G. Halpert, J. Electrochem. Soc. 137 (1990) 2991.

[8] L. Redey, J. Prakash, D.R. Vissers, K.M. Myles, Proc. of 35th International Power Sources Symp., June 22–25, 1992, Cherry Hill, NJ.

[9] J. Prakash, L. Redey, D.R. Vissers, Extended Abstracts, Electrochemical Society Meeting, October 11–16, 1992, Toronto, Canada.

[10] L. Redey, D.R. Vissers, Extended Abstracts, Electrochemical Society Meeting, October 15–20, 1989, Hollywood, FL.

[11] R.J. Bones, J. Coetzer, R.C. Galloway, D.A. Teagle, J. Electrochem. Soc. 134 (1987) 2370.

[12] A Simplified Version of the Federal Urban Driving Schedule for Electric Vehicle Battery Testing, Electric and Hybrid Propulsion Battery Test Working Force, EG&G, Idaho, DOE/ID-10146, Aug. 1988.

[13] L. Redey, in: R.E. White, M.W. Verbrugge, J.F. Stockel (Eds.), Proc. Symp. on Modeling Batteries and Fuel Cells, Electrochemical Society, Pennington, NJ, Vol. 91-10, 1991, p. 122.

[14] L. Redey, in: D.D. MacDonald, A.C. Khandkar (Eds.), Proc. Symp. on High-Temperature Electrode Materials and Characterization, Electrochemical Society, Pennington, NJ, Vol. 91-6, 1991, p. 127.

[15] L. Redey, T. Rauworth, J. Prakash, D.R. Vissers, ECS Meeting, New Orleans, LA, Oct. 1993, Vol. 93-2, Abstr. No. 366, 1993.